



pH influence on oxygen mass transfer coefficient in a bubble column. Individual characterization of k_L and a



A. Ferreira^{a,b,*}, P. Cardoso^b, J.A. Teixeira^a, F. Rocha^b

^a IBB-Institute for Biotechnology and Bioengineering, Centre of Biological Engineering, Universidade do Minho, Campus de Gualtar, 4710-057 Braga, Portugal

^b LEPAE-Laboratory for Process, Environmental and Energy Engineering, Departamento de Engenharia Química, Faculdade de Engenharia, Universidade do Porto, Rua Dr. Roberto Frias s/n, 4200-465 Porto, Portugal

HIGHLIGHTS

- ▶ pH influence on the individual parameters of $k_L a$.
- ▶ $k_L a$ decrease in presence of the common acids and base used in biological process.
- ▶ k_L is strongly influenced by the presence of HCl and KOH.
- ▶ The k_L behavior on the systems was explained based on bubble surface contamination.
- ▶ Information very useful for a better control of biological processes.

ARTICLE INFO

Article history:

Received 29 August 2012

Received in revised form

5 November 2012

Accepted 8 February 2013

Available online 24 February 2013

Keywords:

Bubble columns

Bioreactors

Mass transfer

Multiphase reactors

pH

Bubble surface contamination

ABSTRACT

Experiments were performed in a laboratory scale bubble column (10 L), to investigate the pH influence on oxygen mass transfer coefficient, in order to achieve a better control of biological processes. The liquid-side mass transfer coefficient, k_L , and the specific interfacial area, a , were studied individually. The specific interfacial area was obtained using the new automatic image analysis technique developed by Ferreira et al. (2012). The pH was changed by the addition to the system of the most common acids and base used in biological process: hydrochloric acid (HCl), phosphoric acid (H_3PO_4) and potassium hydroxide (KOH). The results show that aqueous systems containing HCl, H_3PO_4 or KOH present lower volumetric liquid side mass transfer coefficient, $k_L a$, in relation to pure systems (distilled water), this decrease being not linear. It was found that the specific interfacial area presents higher values in KOH and HCl solutions in comparison with distilled water. However, an opposite behavior was observed in the liquid-side mass transfer coefficient values. The k_L behavior on the impure systems was explained based on bubble surface contamination. Higbie's and Frössling's equations were adapted in the present work in order to be used in bubble dispersion systems.

© 2013 Elsevier Ltd. All rights reserved.

1. Introduction

Bubble column reactors are intensively used as multiphase contactors and reactors in chemical, petrochemical, biochemical and metallurgical industries. This kind of reactors can operate in two and three phase systems, the last one being more complex but highly used at the industry. Three-phase bubble column reactors are widely employed in biochemical applications where microorganisms are used as solid suspension. In these reactors, involving microorganisms, the mass transfer from the gas to the

liquid is one of the most important phenomena that can determine the success or failure of the biological process. Mass transfer can be affected by different parameters: gas flow rate, temperature (Ferreira et al., 2010), solids size, density and loading (Su et al., 2006; Mena et al., 2011), liquid properties (Alvarez et al., 2000; Alves et al., 2005; Chaumat et al., 2007), column diameter (Dudley, 1995), sparger design (Kazakis et al., 2008), among others. Regarding the liquid properties, viscosity and surface tension effects on hydrodynamics and bubble characteristics have been investigated in bubble columns over the years (Akita and Yoshida, 1974; Kawase et al., 1987; Hikita et al., 1981; Koide et al., 1984; Deckwer, 1992; Mouza et al., 2005; Orvalho et al., 2009; Maceiras et al., 2010), having a direct repercussion on mass transfer. For example, the decrease in surface tension decreases bubble size and bubble velocity, this inducing higher

* Corresponding author at: IBB-Institute for Biotechnology and Bioengineering, Centre of Biological Engineering, Universidade do Minho, Campus de Gualtar, 4710-057 Braga, Portugal. Tel.: +351 225081678; fax: +351 225081632.

E-mail address: amaf@fe.up.pt (A. Ferreira).

gas holdup and higher mass transfer coefficient (Chaumat et al., 2007). In what concerns the viscosity influence on the mass transfer process, this physical property appears to have a considerable influence on both individual parameters of $k_L a$, according to Ferreira et al. (2012) work. The same authors show that the viscosity has a higher influence on specific interfacial area when compared with surface tension effect.

Surface tension, viscosity, and electrically repulsive forces were also used by Craig et al. (1993) as a possible explanation for the results obtained in their studies related to the electrolytes influence on bubble coalescence. The authors report that only a particular combination of ions can inhibit bubble coalescence. The liquid properties were ruled out as a possible explanation for the observations, however, according to the authors, this phenomenon is mainly related to the electrolyte effect on water structure and hence the hydrophobic interaction. By other way, Weissenborn and Pugh (1995, 1996) explain the contrasting behavior of electrolytes in inhibiting coalescence (combining rule) in terms of positive and negative adsorption of ions at gas/water interface. Further, the efficiency of the electrolytes which inhibit coalescence can be linked to the effect of electrolyte concentration on gas solubility.

In addition, gas–liquid mass transfer between a bubble and surrounding liquid depends upon overall surface mobility, which is affected by contamination by surfactants, or others compounds, and solids. Bubbles with a totally mobile surface present upper values of mass transfer coefficient, k_L , which can be predicted using Higbie's equation (Bird et al., 1960)

$$k_L^{mobile} = 1.13 \sqrt{\frac{u}{d}} D_L^{1/2} \quad (1)$$

where d is the bubble diameter, u is the bubble–liquid relative velocity (slip velocity) and D_L is the diffusivity.

By other way, bubbles with a totally rigid surface present lower k_L values, which can be predicted using an equation proposed by Frössling (1938)

$$k_L^{rigid} = c \sqrt{\frac{u}{d}} D_L^{2/3} \nu^{-1/6} \quad (2)$$

where $c \sim 0.6$ and ν is the kinematic viscosity of the liquid. Based on the bubble contamination kinetics (Alves et al., 2005) develop a simplified stagnant cap model that was used for drag coefficient and gas–liquid mass transfer results interpretation. In this model gas–liquid mass transfer assumes two mass transfer coefficients, one for the clean front of the bubble, and the other for the stagnant cap. According to the authors, adjusted values of these coefficients are consistent with theoretical predictions from Higbie's and Frössling's equations, respectively.

Despite all the research efforts, the knowledge about the effects of the liquid properties on mass transfer remains an open area, especially, in what concerns with its influence on the individual parameters of volumetric liquid side mass transfer coefficient, $k_L a$. In the present work the focus was done to the pH influence on k_L and a in a bubble column. pH is one of the crucial variables that need to be controlled in a biological process in order to maximize the product production (Lee and Tsui, 1999). Therefore, basic or acidic solutions are added to the reactor to neutralize the acids or bases formed during the biological process and keep, by this way, the pH in an optimum biological value. Despite the importance of pH influence on mass transfer in biological processes the data found in the literature are scarce. In order to fill this gap, the pH influence on the individual parameters of volumetric liquid side mass transfer coefficient, $k_L a$, is presented in this work. For that, mass transfer results were combined with the specific interfacial area values obtained

using the new automatic image analysis technique developed by Ferreira et al. (2012).

2. Experimental

2.1. Mass transfer experiments

2.1.1. Experimental set-up

The contact device used to perform the mass transfer experiments was the bubble column represented in Fig. 1(a) with the respective dimensions. The device is a perspex cylindrical column covered by a perspex rectangular box to control the temperature through water circulation. At the bottom a gas chamber is located, where the gas enters first and then passes through a steel sparger, with a thickness of 2 mm, where the bubbles are formed. The sparger has a relative free area of 0.05% for a orifice diameter of 0.5 mm (Fig. 1(b)).

2.1.2. Methodology

Oxygen mass transfer experiments were performed in two-phase system at constant temperature (25 °C) and different superficial gas velocities (up to 14 mm/s) and system pH. The pH was changed in order to increase the acidity or alkalinity of the system through the addition of hydrochloric acid (HCl 37%, Merck), phosphoric acid (H₃PO₄ 85%, Merck) or potassium hydroxide (KOH, Merck) (the most common acids and base used in biological process). Air K was used as gas phase. The liquid height was $h_0 = 0.65$ m for all experiments (no liquid throughput). Table 1 presents a summary of the experimental conditions used in the present work.

Initially the liquid is deoxygenated by bubbling nitrogen. When the dissolved oxygen concentration is practically zero, humidified air is fed into the column. At this moment the oxygen transfer process from bubbles to the liquid begins and continues until oxygen concentration in the liquid reaches the saturation. Dissolved oxygen concentration values were measured online using an O₂ electrode (Cellox 325, WTW), located 0.20 m from the gas sparger and 0.07 m from the wall, connected to a DO-meter with resolution 0.01 mg/L or 0.1% saturation (WTW OXI 340), and recorded directly in a PC, through a data acquisition board. No bubbles interference on the probe measurements was observed. By this way, the dissolved oxygen concentration variation with time, t , is obtained, and $k_L a$ can be calculated according to the following procedure.

The mass balance for oxygen in the liquid is written as

$$\frac{dC}{dt} = k_L a (C^* - C) \quad (3)$$

where C^* and C are, respectively, the oxygen solubility and oxygen concentration in the liquid. Assuming the liquid phase homogeneous and C_0 the oxygen concentration at $t=0$, the integration of the previous equation leads to

$$\ln(C^* - C) = \ln(C^* - C_0) - k_L a \cdot t \quad (4)$$

The volumetric mass transfer coefficient can now be determined by plotting $\ln(C^* - C)$ against time (t).

Typically, the dissolved oxygen concentration during the aeration has two distinguished zones, one with an intense mass transfer zone where the O₂ concentration rises fast and other close to the saturation, when the mass transfer rate starts to decline. As previously mentioned, plotting $\ln(C^* - C)$ against time, $k_L a$ can be determined from the slope in the linear zone. In order to define this zone by a statistic way, the statistical method *Test F* (Hoel, 1976) was used. This method consists in the determination of the optimum number of points (n_p) for a linear regression of

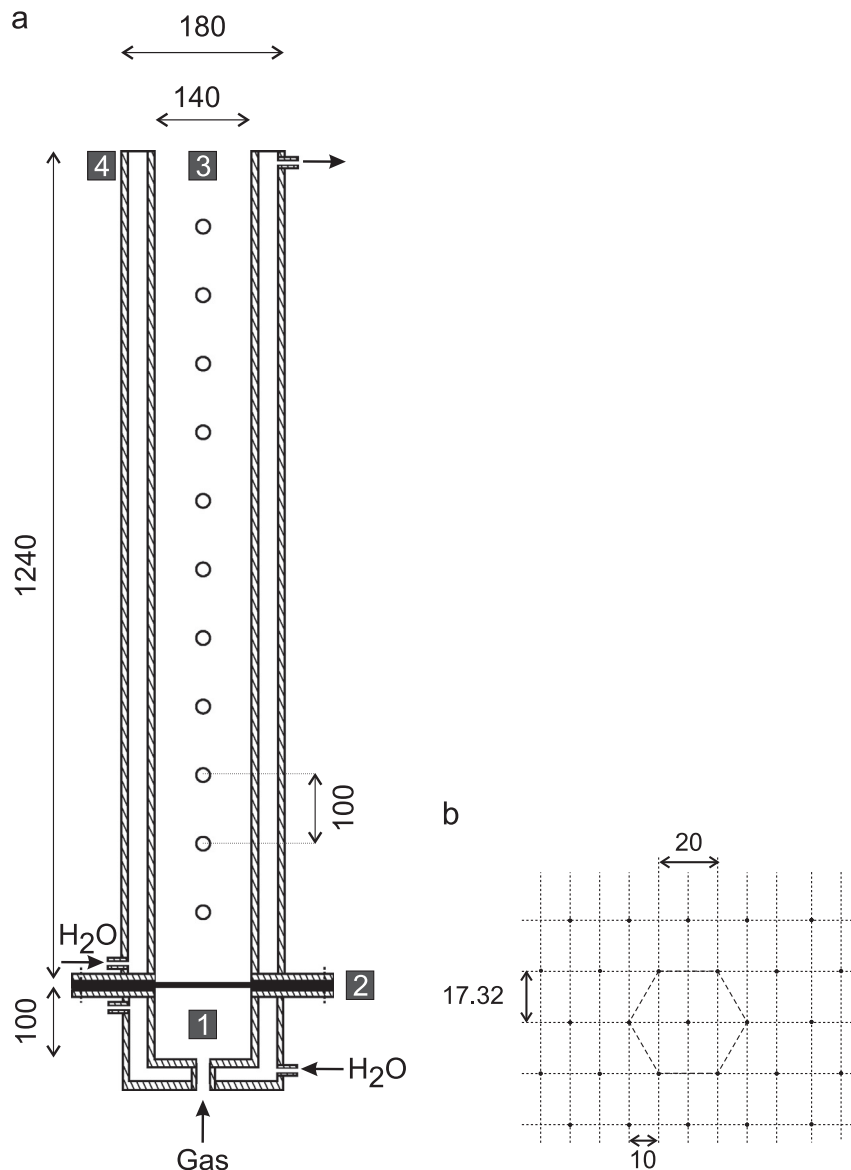


Fig. 1. Bubble column (a) and sparger (b) used in the present work (all dimensions in mm): 1, gas chamber; 2, sparger; 3, cylindrical column; 4, rectangular box.

Table 1

Experimental conditions used in the present work.

Liquid phase			Gas phase
Type	pH	T ($^{\circ}\text{C}$)	$u_G \times 10^3$ (m/s)
Distilled water	6.7	25	Up to 14
Distilled water + HCl	$3.1 < \text{pH} < 6.7$	25	Up to 14
Distilled water + H_3PO_4	$3.1 < \text{pH} < 6.7$	25	Up to 14
Distilled water + KOH	$6.7 < \text{pH} < 10.4$	25	Up to 14

experimental data (Mena et al., 2011). The solubility of oxygen in water (C^*) was taken experimentally for each run.

The experimental results are reproducible with an average relative error of 5% and are not influenced by the dynamics of the oxygen electrode since its response time, less than 16 s for a 95% confidence interval (technical data), was much smaller than the mass transfer time of the system (ranging from 35 to 120 s). The first-order time constant of this probe, measured by Vasconcelos et al. (2003), presents the value of ~ 6 s, indicating, by this way, its possible application in the present system. The claimed

average relative error of 5% was calculated from five runs (at same conditions) in pure systems; replicate experiments were done for the impure systems and the results obtained are reproducible, inside the error obtained for the pure system.

2.2. Image analysis experiments

In order to obtain the bubble size distribution and, consequently, the specific interfacial area a , a second experimental setup was used, Fig. 2. The device is a perspex rectangular column ($W \times D \times H$: 140 mm \times 20 mm \times 1240 mm) covered by a perspex rectangular box to control the temperature through water circulation and to minimize the optical distortion. The column was designed in order to minimize the problems related with the effect of bubble position in the column on bubble size measurement using image analysis techniques. By this way, it was possible to reduce the error, associated to this effect, for a value less than 3% (value obtained using a scale cover glass with a 7 mm (diameter) circle positioned in the column at different distances from the wall; the images obtained were automatically treated using the methodology developed by Ferreira et al., 2012).

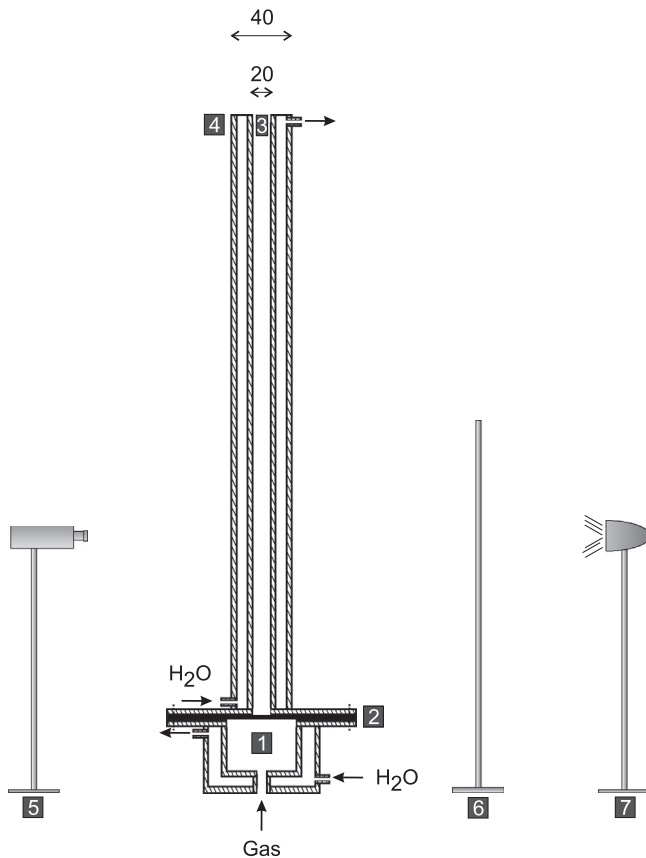


Fig. 2. Experimental set-up for visualization measurements (all dimensions in mm): 1, gas chamber; 2, sparger; 3, rectangular column ($W \times D \times H$: 140 mm \times 20 mm \times 1240 mm); 4, rectangular box; 5, digital camera; 6, diffuser glass; 7, halogen lamp.

Moreover, no influence on bubble size and shape was verified using this rectangular column in comparison with the bubble column used in mass transfer experiments (Ferreira et al., 2012). A gas chamber is located at the bottom where the gas enters first and then passes through a steel sparger, with a thickness of 2 mm, where the bubbles are formed. The sparger is constituted by a single line of orifices (diameter of 0.5 mm) with a pitch of 20 mm and a relative free area of 0.05%. Sets of images, obtained 0.4 m from the gas sparger, were grabbed with a black and white high speed digital video camera (frame rate of 250 images/s) connected to a PC, and used to study the bubble shape and size in the same conditions of $k_L a$ determinations. After the acquisition a set of images (about 5 images/s) are automatically treated and the bubbles are identified and classified according to the methodology developed by Ferreira et al. (2012). With the previous methodology, the automatic identification of single bubbles (isolated bubbles without influence of surrounded bubbles) in the studied systems was possible. The automatic and correct characterization of the single bubbles allows the correct determination of bubble size and, consequently, the specific interfacial area a .

As the shape of the bubbles is influenced by the superficial velocity and, usually, these present a spheroid geometry (Mena et al., 2005a), the size of each individual bubble (D_{eq_i}) was determined from the superficial area of the bubble (A_{sup_i}) according to the following equation:

$$D_{eq_i} = 2\sqrt{A_{sup_i}/4\pi} \quad (5)$$

where

$$A_{sup_i} = 2\pi r_1^2 + \pi r_1 r_2 \ln\left(\frac{r_1 + r_2}{r_1 - r_2}\right)$$

and, $2r_1$ and $2r_2$ correspond to the maximal Feret diameter and minimal Feret diameter, respectively (Ferreira et al., 2012).

For processes involving mass transfer through an interfacial area, the bubble size distribution (BSD) is well represented by the Sauter mean diameter (d_{32}) which is given by

$$d_{32} = \frac{\sum_i n_i \cdot D_{eq_i}^3}{\sum_i n_i \cdot D_{eq_i}^2} \quad (6)$$

The specific interfacial area, a , can be determined from the gas hold-up, ε_G , and the BSD as follows:

$$a = 6 \frac{\varepsilon_G}{d_{32}} \quad (7)$$

The volume fraction of the gas phase was measured by bed expansion with a relative error less than 7.5%. The claimed error is the upper limit for voidage error in the range measured. As the liquid layer is uniform, stable and horizontal surface, the interface can be located with precision of 1 mm (resolution of the ruler). For layers with liquid height (h) \approx 66.3–71.5 cm (voidage 2–10%), this gives an error of 0.15–0.14% in h which causes an error of 7.5–1.5%, respectively, in ε_G .

3. Results and discussion

3.1. HCl, H₃PO₄ and KOH influence on $k_L a$

In Fig. 3(a) the experimental results, obtained in the present work at 25 °C for pure system, are compared with some literature correlations. These were chosen taking into account the ones that include some liquid properties (e.g. diffusivity, viscosity, interfacial tension, etc.). No correlation related to pH influence on $k_L a$ was found in the literature. As one can see, most of the correlations underestimate the experimental values, probably due to differences in the experimental conditions, mainly in superficial gas velocity range. Kawase et al. (1987), Hikita et al. (1981) and Koide et al. (1984) works present superficial gas velocities above 0.02 m/s, while Akita and Yoshida (1973) worked in the range of 0.003–0.4 m/s. In all of these works the correlations were obtained mostly in heterogenous regime (the superficial gas velocities used were higher than the upper limit of 0.04 m/s for the homogeneous flow regime in pure system Mena et al., 2005b) presenting by this way low values when extrapolated for the homogeneous regime. On the other hand, the present results are very similar to the ones obtained by Vasconcelos et al. (2003), that worked just inside the homogeneous regime.

In what concerns the concentration effect of HCl, H₃PO₄ and KOH on $k_L a$ the main results are presented in Fig. 3(b)–(d). As one can see, mass transfer decreases in the presence of all compounds. According to Fig. 4 a maximum and a minimum are observed for $k_L a$ at different pHs and systems. Regarding the acids influence, it seems that HCl has a higher influence on $k_L a$ presenting a maximum influence on two different pHs, according to the superficial gas velocity used. For $u_G < 0.9$ cm/s the maximum influence on the mass transfer process was observed at pH=4.4, while for superficial gas velocities above 0.9 cm/s this value changes to pH=3.5. In the H₃PO₄ system, this behavior, the existence of $k_L a$ minimum values, was not so evident. According to Craig et al. (1993) big differences between HCl and H₃PO₄ are not expected, as these systems present the same coalescence behavior. So, the previous results just can be related with k_L variation. By this way, it is expected that systems contaminated

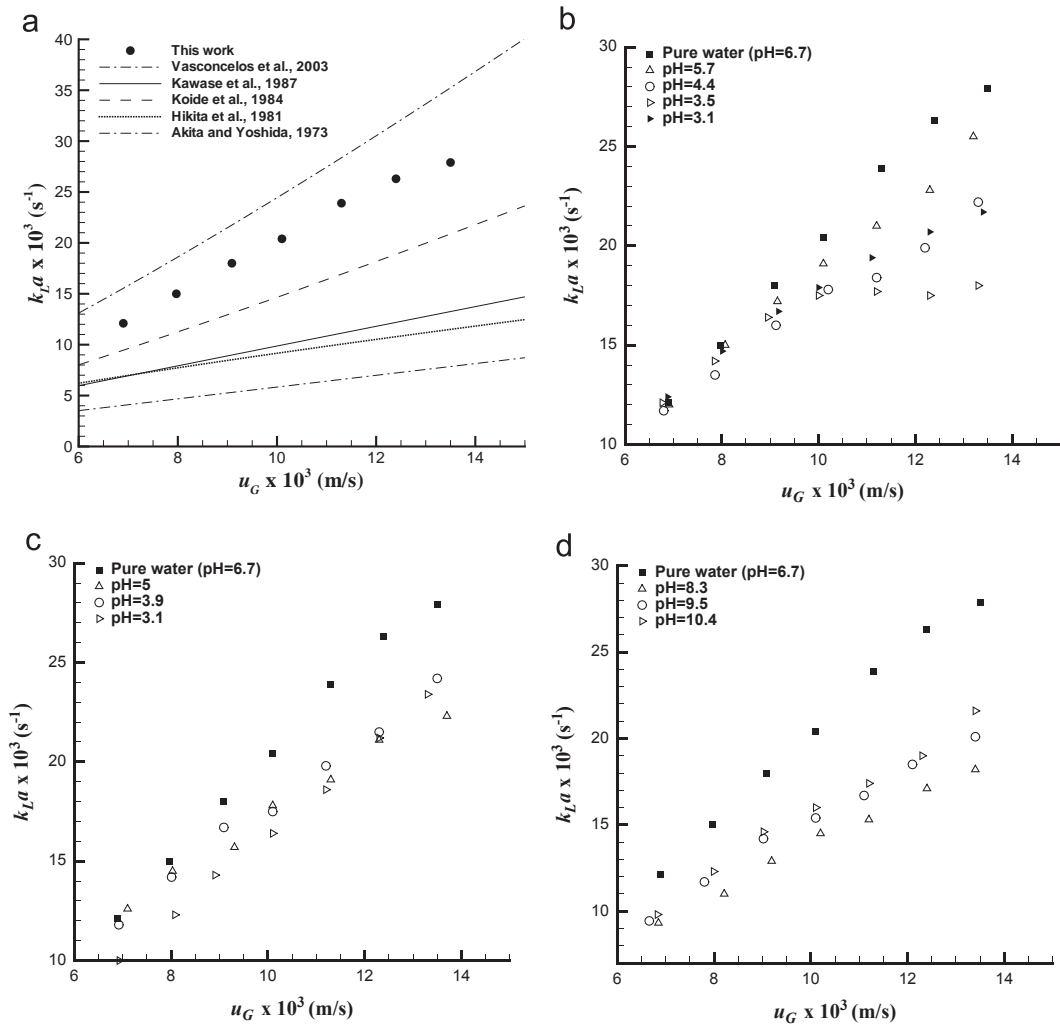


Fig. 3. Experimental volumetric liquid-side mass transfer coefficient ($k_L a$) and literature correlations for air/water system (a) and the effect of HCl (b), H₃PO₄ (c) and KOH (d) on $k_L a$, at 25 °C.

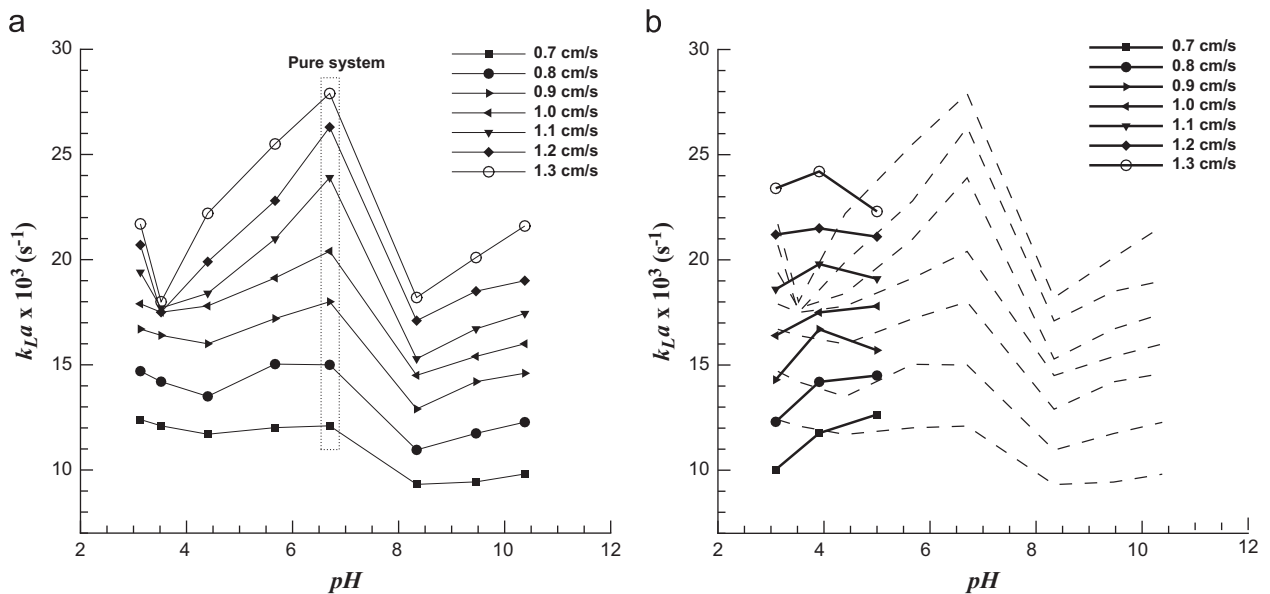


Fig. 4. pH influence on volumetric liquid-side mass transfer coefficient at 25 °C for different superficial gas velocities. H₂O/HCl and H₂O/KOH systems (a); H₂O/H₃PO₄ system, the dashed lines show the H₂O/HCl and H₂O/KOH systems (b).

with HCl present less k_L values, probably related to a higher bubble surface contamination. This subject will be discussed in Section 3.2.

In what concerns the KOH influence, it seems that low concentration induces a higher $k_L a$ decrease. However, as we increase the base concentration a $k_L a$ increase is observed. This effect is probably related to the bubble coalescence reduction. According to Craig et al. (1993) the basicity increase leads to a higher balance between bubble coalescence and break resulting in a bubble size reduction and, consequently, on a higher a and mass transfer.

According to the previous results analysis, knowledge about the influence of pH on mass transfer process falls in the studies of the individual parameters of $k_L a$.

3.2. HCl and KOH influence on k_L and a

In order to evaluate the pH influence on the individual parameter of $k_L a$ several image analysis experiments were performed using the methodology developed by Ferreira et al. (2012). The pH and systems chosen were: pH=3.5 using HCl and pH=10.4 using KOH. On the acidic part it was chosen the acid with higher impact on mass transfer, i.e. HCl.

As previous reported both, HCl and KOH, have a high impact on mass transfer process. For the pHs under study on this section

KOH decreases $k_L a$ for all superficial gas velocities (Fig. 5(a)). By other way, HCl seems not to have any influence for low gas velocities (less than 0.9 cm/s), however for higher velocities the “impurity” almost stop the mass transfer in a constant value.

3.2.1. Influence on the specific interfacial area, a

According to Craig et al. (1993) work a positive impact on a using KOH is expected, as this compound decreases the bubble coalescence. On the other hand, no influence on a is expected when HCl is used. Based on Weissenborn and Pugh (1995, 1996) works no difference between HCl and KOH is expected under the concentrations studied, as no significant differences on liquid properties are observed, specially in what concerns the dissolved gas (microbubbles) gradients between macroscopic bubbles, a parameter that is responsible, according to the authors, for the inhibition of coalescence.

Thus, based on the previous works, it is expected a small increase on a when KOH is used and no variation is expected when HCl is added to the system. In order to verify these conclusions a was determined at different experimental conditions. For that, gas holdup, ε , and d_{32} were used, Fig. 5(b) and (c), respectively. As one can see the impure systems increase the gas holdup for the superficial gas velocities above 0.9 cm/s, this being related to the bubble size decrease. Applying Eq. (7), the a

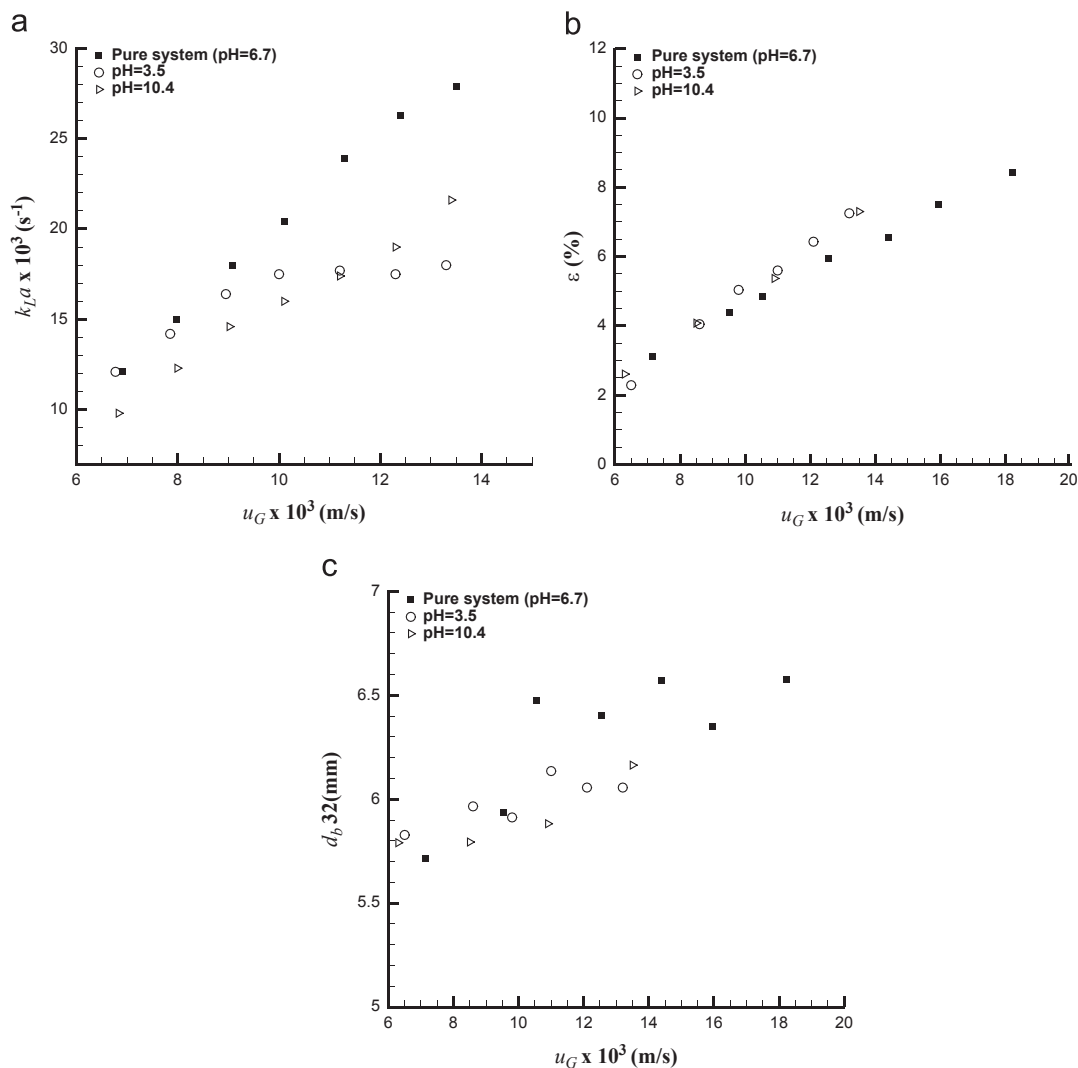


Fig. 5. Dependence of $k_L a$ (a), gas holdup (ε) (b) and d_{32} (c) on superficial gas velocity for pure and impure systems.

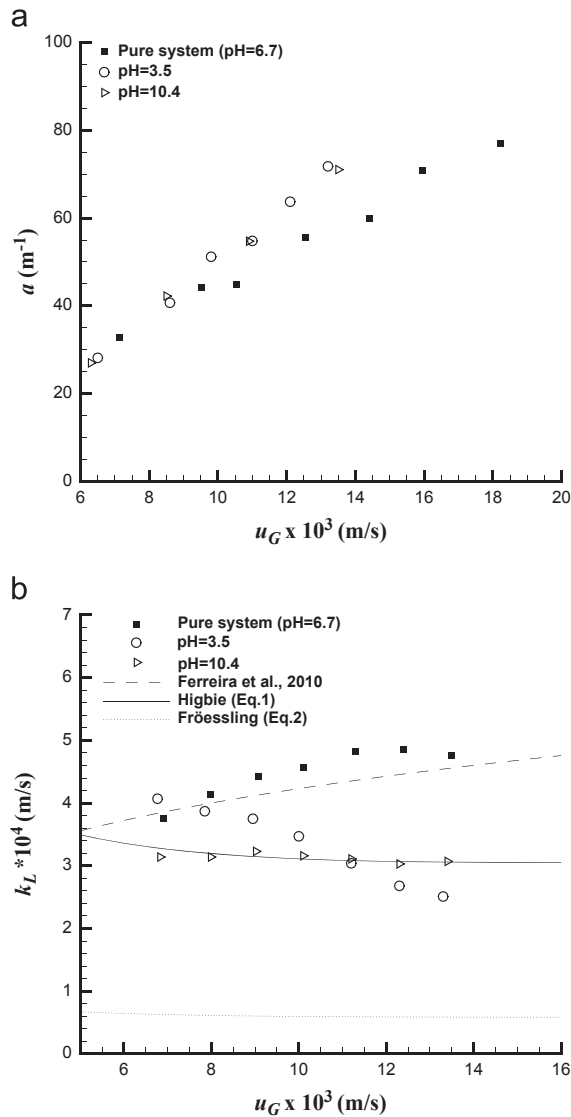


Fig. 6. Dependence of interfacial area (a) and liquid-side mass transfer coefficient (b) on superficial gas velocity for pure and impure systems.

variation with the superficial gas velocity on the different systems is obtained, Fig. 6(a). As one can see the “impurities” increase the interfacial area when the system is operating at superficial gas velocities above 0.9 cm/s, confirming the literature results for the KOH system. On the other hand, the HCl influence on a was not expected.

Based on a experimental results, a mass transfer increase in all systems, specially for higher velocities, was expected. Such was not observed. Thus, k_L seems to play a crucial role on those systems.

3.2.2. Influence on the liquid-side mass transfer coefficient, k_L

As no significant influences on liquid properties are expected, in the systems studied, the HCl and KOH influence on $k_L a$ falls on bubble surface contamination. Alves et al. (2005) developed a simplified stagnant cap model that was used for gas–liquid mass transfer interpretation assuming two mass transfer coefficients, one for the clean front of the bubble (predicted by Eq. (1), the other for the stagnant cap (predicted by Eq. (2)). In Fig. 6(b) the k_L variation in the different systems is presented, as well as the prediction based on Higbie’s and Frössling’s

equations and literature results. As one can see the k_L variation in the pure system is not well predicted by the Higbie’s equation, only for low velocities some concordance can be observed. This observation was expected, as the theoretical predictions are based on single bubbles studies and their application on bubble swarms usually fails. On the other hand, their application to isolated bubbles studies can be very useful, as one can see by the Higbie’s equation and Vasconcelos et al. (2002) results comparison. According to the literature (Koynov et al., 2005; Martín et al., 2009; Ferreira et al., 2012) the influence of the other bubbles on the individual bubbles is an important task on mass transfer process. So, the k_L obtained for one single bubble cannot be used as an absolute value in a bubbles dispersion because of the presence of other bubbles in the system. Ferreira et al. (2012) have shown that in these systems the turbulence produced by close bubbles and the bubble size are some of the most important parameters that rule the mass transfer process. So, the application of some conclusions obtained on single bubbles studies into bubble swarms need to be done carefully. In the present study we can infer that only for low velocities, where the bubbles flow almost individually without influence of other bubbles, the theoretical models can be applied. As we increase the superficial gas velocity a deviation from the theoretical prediction is observed. In these conditions the equation obtained by Ferreira et al. (2010) seems to predict well the k_L behavior, however, this equation cannot be used when the bubble surface contamination starts to be the predominant parameter on mass transfer control. Thus, the impure systems presented in this work were discussed according to the theoretical predictions of Higbie’s and Frössling’s equations. In order to adapt both equations to the bubble swarm systems Ferreira’s and Higbie’s equations were compared. Analyzing the data obtained by both equations for the superficial gas velocities under study one can infer that the average difference of k_L obtained in bubble swarms and the one obtained in single bubbles experiments is about 40%. So, and assuming that the differences of Higbie’s and Frössling’s equations remain constant in bubble swarms, a factor of 1.4 and 3.4, respectively, was applied to the previous equations, in order to be used in bubble dispersion systems. Analyzing Fig. 7 it can be concluded that the superficial gas velocity increase induces a bubble surface contamination in the HCl system, the last k_L values being close to the ones predicted by the “new” Frössling’s equation. This

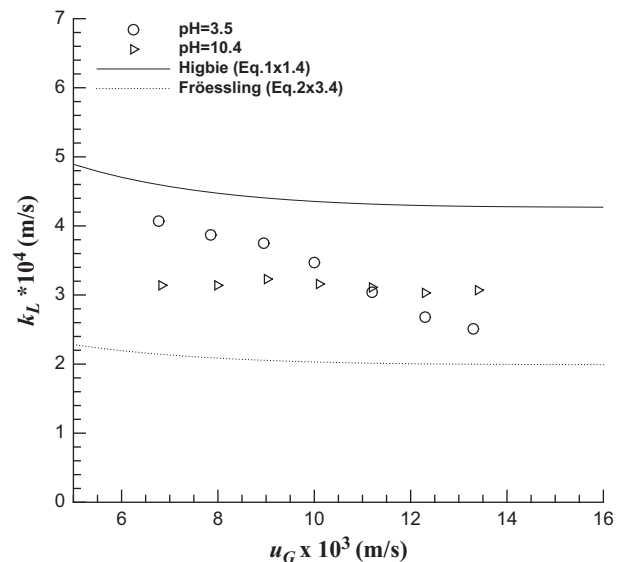


Fig. 7. Dependence of liquid-side mass transfer coefficient on superficial gas velocity at different pHs.

observation is probably related to the system turbulence increase with the superficial gas velocity (Ferreira et al., 2012). In what concerns the KOH influence on k_L , it seems that superficial gas velocity does not play any role on that. In these systems the turbulence seems do not change the bubble surface contamination.

4. Conclusions

The gas–liquid mass transfer process was investigated in a two-phase bubble column at different pHs. The main purpose was to analyze the pH influence on the individual parameters of volumetric liquid side mass transfer coefficient, $k_L a$, in order to help some decisions in biological processes control.

The results show that aqueous systems containing HCl, H₃PO₄ or KOH present less $k_L a$ values, in relation to pure systems (distilled water). HCl and KOH present the highest impacts on the mass transfer process, these being related with a high decrease of k_L . The liquid-side mass transfer coefficient seems to be connected with bubble surface contamination. Higbie's and Frössling's equations, adapted in the present work in order to be used in bubble dispersion systems, have been successfully applied in describing the bubble surface contamination. However, more deep studies, regarding the surface contamination in bubble swarms, need to be done. Regarding the specific interfacial area, it was found that a presents higher values in KOH and HCl solutions in comparison with distilled water, these observations being in agreement with the literature for the KOH system.

In short, the pH selection on biological processes as well as the compound, or compounds, used for that pH control, need to take into account their effects on the individual parameter of $k_L a$. A selection only based on a measurements can result in a bad option.

Nomenclature

A_{proj}	projected bubble area (m ²)
A_{sup_i}	bubble superficial area (m ²)
a	specific interfacial area (m ⁻¹)
C	oxygen concentration in the liquid (kg/L)
C_0	oxygen concentration in the liquid at $t=0$ (kg/L)
C^*	oxygen solubility in the liquid (kg/L)
D_{eq}	equivalent diameter (m)
D_L	diffusivity of gas in the liquid (m ² /s)
d	bubble diameter (m)
d_{32}	Sauter mean diameter (m)
h	liquid height (m)
h_0	initial liquid height (m)
k_L	liquid-side mass transfer coefficient (m/s)
$k_{L,a}$	volumetric liquid side mass transfer coefficient (s ⁻¹)
T	temperature (°C)
t	time (s)
u	bubble–liquid relative velocity (slip velocity) (m/s)
u_G	superficial gas velocity (m/s)
ε_G	gas holdup, dimensionless
ν	kinematic viscosity (m ² /s)

Acknowledgments

This work was supported by Fundação para a Ciência e Tecnologia under program contract number SFRH/BPD/45637/2008.

References

- Akita, K., Yoshida, F., 1973. Gas holdup and volumetric mass transfer coefficient in bubble columns. Effects of liquid properties. *Ind. Eng. Chem. Process Des. Dev.* 12 (1), 76–80.
- Akita, K., Yoshida, F., 1974. Bubble size, interfacial area, and liquid-phase mass transfer coefficient in bubble columns. *Ind. Eng. Chem. Process Des. Dev.* 13 (1), 84–91.
- Alvarez, E., Sanjurjo, B., Cancela, A., Navaza, J.M., 2000. Mass transfer and influence of physical properties of solutions in a bubble column. *Chem. Eng. Res. Des.* 78, 889–893.
- Alves, S., Orvalho, S., Vasconcelos, J., 2005. Effect of bubble contamination on rise velocity and mass transfer. *Chem. Eng. Sci.* 60 (1), 1–9.
- Bird, R.B., Stewart, W.E., Lighfoot, E.N., 1960. *Transport Phenomena*. Wiley New York.
- Chaumat, H., Billet, a.M., Delmas, H., 2007. Hydrodynamics and mass transfer in bubble column: influence of liquid phase surface tension. *Chem. Eng. Sci.* 62 (24), 7378–7390.
- Craig, V.S.J., Ninham, B.W., Pashley, R.M., 1993. The effect of electrolytes on bubble coalescence in water. *J. Phys. Chem.* 97 (39), 10192–10197.
- Deckwer, W.D., 1992. *Bubble Column Reactors*. J. Wiley.
- Dudley, J., 1995. Mass transfer in bubble columns: a comparison of correlations. *Water Res.* 29 (4), 1129–1138.
- Ferreira, A., Ferreira, C., Teixeira, J., Rocha, F., 2010. Temperature and solid properties effects on gas–liquid mass transfer. *Chem. Eng. J.* 162 (2), 743–752.
- Ferreira, A., Pereira, G., Teixeira, J., Rocha, F., 2012. Statistical tool combined with image analysis to characterize hydrodynamics and mass transfer in a bubble column. *Chem. Eng. J.* 180, 216–228.
- Frössling, N., 1938. Über die verdunstung fallenden tropfen (Evaporation of falling drops). *Gerl. Beitr. Geophys.* 52, 170–216.
- Hikita, H., Asai, S., Kikukawa, H., Zalke, T., Ohue, M., 1981. Heat transfer coefficient in bubble column. *Ind. Eng. Chem. Process Des. Dev.* 20, 540–545.
- Hoel, P.G., 1976. *Elementary Statistics*, 4th edition John Wiley & Sons Inc., Australia.
- Kawase, Y., Halard, B., Moo-Young, M., 1987. Theoretical prediction of volumetric mass transfer coefficients in bubble columns for newtonian and non-newtonian fluids. *Chem. Eng. Sci.* 42 (7), 1609–1617.
- Kazakis, N., Mouza, a.a., Paras, S., 2008. Experimental study of bubble formation at metal porous spargers: effect of liquid properties and sparger characteristics on the initial bubble size distribution. *Chem. Eng. J.* 137 (2), 265–281.
- Koide, K., Takazawa, A., Komura, M., Matsunga, H., Matsunaga, H., 1984. Gas holdup and volumetric liquid-phase mass transfer coefficient in solid-suspended bubble columns. *J. Chem. Eng. Jpn.* 17, 459.
- Koynov, A., Khinast, J.G., Tryggvason, G.A., 2005. Mass transfer and chemical reactions in bubble swarms with dynamic interfaces. *AIChE J.* 51 (10), 2786–2800.
- Lee, S.-Y., Tsui, Y.P., 1999. Succeed at gas/liquid contacting. *Chem. Eng. Prog.* 95 (7), 23–49.
- Maceiras, R., Álvarez, E., Cancela, M., 2010. Experimental interfacial area measurements in a bubble column. *Chem. Eng. J.* 163 (3), 331–336.
- Martín, M., Montes, F.J., Galán, M.a., 2009. Mass transfer from oscillating bubbles in bubble column reactors. *Chem. Eng. J.* 151 (1–3), 79–88.
- Mena, P., Ferreira, A., Teixeira, J.A., Rocha, F., 2011. Effect of some solid properties on gas–liquid mass transfer in a bubble column. *Chem. Eng. Process.: Process Intensification* 50 (2), 181–188.
- Mena, P.C., Pons, M.C., Teixeira, J.A., Rocha, F.A., 2005a. Using image analysis in the study of multiphase gas absorption. *Chem. Eng. Sci.* 60 (18), 5144–5150.
- Mena, P.C., Rocha, F.A., Teixeira, J.A., Drahos, J., Ruzicka, M.C., Drahoš, J., 2005b. Effect of solids on homogeneous–heterogeneous flow regime transition in three-phase bubble columns. *Chem. Eng. Sci.* 60 (22), 6013–6026.
- Mouza, A.A., Dalakoglou, G.K., Paras, S.V., 2005. Effect of liquid properties on the performance of bubble column reactors with fine pore spargers. *Chem. Eng. Sci.* 60 (5), 1465–1475.
- Orvalho, S., Ruzicka, M.C., Drahos, J., 2009. Bubble column with electrolytes: gas holdup and flow regimes. *Ind. Eng. Chem. Res.* 48, 8237–8243.
- Su, X., Hol, P.D., Talcott, S.M., Staudt, A.K., Heindel, T.J., 2006. The effect of bubble column diameter on gas holdup in fiber suspensions. *Chem. Eng. Sci.* 61 (10), 3098–3104.
- Vasconcelos, J.M.T., Orvalho, S.P., Alves, S.a.S., 2002. Gas–liquid mass transfer to single bubbles: effect of surface contamination. *AIChE J.* 48 (6), 1145–1154.
- Vasconcelos, J.M.T., Rodrigues, J.M.L., Orvalho, S.C.P., Alves, S., Mendes, R.L., Reis, A., 2003. Effect of contaminants on mass transfer coefficients in bubble column and airlift contactors. *Chem. Eng. Sci.* 58 (8), 1431–1440.
- Weissenborn, P.K., Pugh, R.J., 1995. Surface tension and bubble coalescence phenomena of aqueous solutions of electrolytes. *Langmuir* 11 (5), 1422–1426.
- Weissenborn, P.K., Pugh, R.J., 1996. Surface tension of aqueous solutions of electrolytes: relationship with ion hydration, oxygen solubility, and bubble coalescence. *J. Colloid Interf. Sci.* 184, 550–563.